Estimation of Compressive Strength of Activated Binary Cement Mortars Using Response Surface Methodology and Artificial Neural Networks

Saida BOUALLEG [1], Mohamed Aziz CHIKOUCHE [1], Abdesselam BOUIRI [2] *, Malika CHENNA [3], Abdelkader DJERAD [4], Laid BAALI [1]

[1] *Laboratory of Materials and Structural Mechanics (LMMS), Department of Civil Engineering, Faculty of Technology, University of M'sila, University Pole, Bordj Bou Arreridj Road, M'sila 28000, Algeria*
[2] *Faculty of Science and Technology, University of Tindouf, Algeria*
[3] *MDD Lab, University of Bouira, Department of Science and Technology, Faculty of Technology, University Pole, Bordj Bou Arreridj Road, M'sila 28000, Algeria*
[4] *Laboratory of Pure and Applied Mathematics, Department of Mathematics, Faculty of Mathematics, University Pole, Bordj Bou Arreridj Road, M'sila 28000, Algeria*

http://doi.org/10.5755/j02.ms.45203

Received 5 June 2026; accepted 6 August 2026

This study investigates the prediction of the compressive strength of activated binary cement mortars containing ground granulated blast-furnace slag (GGBFS) using two complementary modelling approaches: response surface methodology (RSM) and an artificial neural network (ANN). A database of 96 mix-curing combinations was assembled from the published literature on activated slag cement systems. Four input parameters were considered: slag replacement ratio (0 – 70 %), slag fineness (Blaine, 320 – 650 m²/kg), curing temperature (20 – 80 °C) and curing time (1 – 90 days). The output variable was the 1- to 90-day compressive strength (9 – 64 MPa). A second-order RSM polynomial was fitted and analysed by ANOVA, while a back-propagation feed-forward ANN with a 4-9-6-1 architecture and hyperbolic tangent activation was trained using the Levenberg–Marquardt algorithm with early stopping. The ANN reached $R^2 = 0.991$ and RMSE = 1.39 MPa over the whole dataset, clearly outperforming the RSM model ($R^2 = 0.785$, RMSE = 6.83 MPa). Sensitivity analysis showed that curing time was the dominant predictor (66 %), followed by slag fineness (22 %), curing temperature (6 %), and slag replacement ratio (5 %). The results confirm that ANN is a more reliable surrogate for the highly non-linear hydration kinetics of activated slag mortars and can be used to support mix-design decisions and reduce experimental effort.

Keywords: compressive strength, activated slag mortar, response surface methodology, artificial neural network, sensitivity analysis, mechanical activation, thermal activation.

1. INTRODUCTION

Concrete and cement-based mortars remain the backbone of the global construction industry, yet ordinary Portland cement (OPC) production is responsible for approximately 7 – 8 % of anthropogenic CO_2 emissions [1, 8]. To improve the environmental profile of cementitious composites, supplementary cementitious materials (SCMs) such as ground granulated blast-furnace slag (GGBFS), fly ash, silica fume and metakaolin are increasingly used as partial replacements for OPC. Among these, GGBFS is particularly attractive because it is an abundant industrial by-product whose latent hydraulic activity can be triggered by chemical, mechanical or thermal activation, leading to binders that often match or exceed the long-term mechanical performance of pure OPC systems [1, 8].

The compressive strength (fc) of activated binary slag–OPC mortars is governed by a strongly non-linear interaction between mix-design variables (cement-to-binder ratio, slag replacement level, water-to-binder ratio) and curing conditions (temperature, relative humidity, age). Conventional regression analysis frequently fails to capture this non-linearity, especially when the dataset spans wide ranges of slag replacement and curing regimes [1, 2].

Soft-computing techniques have therefore become a popular alternative for predicting the mechanical properties of cementitious composites. Apostolopoulou et al. [1] developed a back-propagation neural network (BPNN) trained on 298 cement- and lime-metakaolin specimens and reported a global correlation coefficient $R = 0.998$ with an a20-index of 0.93. Li et al. [2] compared an artificial neural network (ANN), an adaptive neuro-fuzzy inference system (ANFIS), and a response-surface methodology (RSM) model on 324 high-strength concrete samples and showed that the ANN ($R^2 = 0.998$) outperformed both ANFIS ($R^2 = 0.926$) and RSM ($R^2 = 0.963$), with cement and fine-aggregate content emerging as the most influential variables. Al-Jamimi et al. [3] coupled a support vector machine with a genetic algorithm (SVM-GA) for plain and blended cement concretes and reached $R^2 = 0.99$ on the test set, confirming the ability of hybrid intelligent models to handle the nonlinearity of OPC–SCM systems.

Despite this progress, the literature on data-driven prediction of activated slag mortars specifically, that is, mortars in which slag is the dominant binder and is activated

* Corresponding author: A. Bouri
E-mail: *abdesselam.bouiri@cuniv-tindouf.dz*

mechanically (by increasing fineness) or thermally (by elevated curing temperature), is still limited. Most published studies focus on either OPC concretes [2, 3] or lime-based historic mortars [1]. Yet the dual mechanical/thermal activation of slag introduces additional non-linearity and synergy effects that are not well captured by classical regression equations.

This work addresses that gap by developing two complementary surrogate models, a quadratic RSM polynomial and a back-propagation ANN, for predicting the compressive strength of activated binary slag – OPC mortars. Four physically meaningful input variables are considered: slag replacement ratio, slag fineness (Blaine), curing temperature, and curing age. The objectives of the study are to build a unified database covering the full activation domain reported in the literature; fit and validate an RSM second-order model with full ANOVA; train and validate a feed-forward ANN; compare the two models in terms of accuracy and engineering robustness; and rank the input variables by their relative importance using a model-based sensitivity analysis.

2. MATERIALS AND EXPERIMENTAL DATABASE

2.1. Materials

The mortars considered in this work are binary activated systems composed of CEM I 42.5 R Portland cement (PC) and ground granulated blast-furnace slag (GGBFS) with a chemical composition typical of European slags ($CaO \approx 38-43$ %, $SiO_2 \approx 32-37$ %, $Al_2O_3 \approx 10-13$ %, $MgO \approx 6-10$ %). The fine aggregate was siliceous standard sand conforming to EN 196-1, used at a constant binder-to-sand ratio of 1:3, and the water-to-binder (w/b) ratio was kept at 0.50 in all reference mixes. Mechanical activation of the slag was achieved by varying the Blaine fineness between 320 and 650 m²/kg, and thermal activation was applied through controlled curing at 20, 40, 60 and 80 °C up to 90 days [1, 3].

2.2. Variables and database

Following the methodology used by Apostolopoulou et al. [1], who compiled an experimental database of 298 specimens from nine independent literature sources, a unified database of 96 mix-curing combinations was assembled in this work from published studies on activated binary slag mortars. Each record contains the four independent variables listed below and the corresponding compressive strength at the given curing age measured on cubic specimens (40×40×40 mm) according to EN 1015-11.

- slag replacement ratio, S (% of total binder), 0 – 70 %;
- slag Blaine fineness, B (m²/kg), 320 – 650 m²/kg (mechanical activation);
- curing temperature, T (°C), 20 – 80 °C (thermal activation);
- curing age, t (days), 1 – 90 days.

The output variable is the cube compressive strength f_c ranging from 9.3 to 63.5 MPa across all records. Descriptive statistics of the database are summarised in Table 1, and the corresponding histograms are shown in Fig. 1.

As shown in Fig. 2, the curing age exhibits the strongest linear correlation with the compressive strength ($\rho \approx 0.63$), followed by the Blaine fineness ($\rho \approx 0.22$), whereas the curing temperature shows practically no linear correlation with strength ($\rho \approx 0.04$), its effect being essentially non-linear and coupled with age.

Table 1. Descriptive statistics of the input and output variables of the activated slag mortar database (N = 96)

Variable	Units	Min	Mean	Max	SD
Slag replacement	%	0.0	36.15	70.0	21.69
Blaine fineness	m²/kg	320	480.83	650	108.44
Curing temperature	°C	20	50.42	80	22.85
Curing age	days	1	22.43	90	28.07
Compressive strength	MPa	9.34	33.89	63.54	14.82

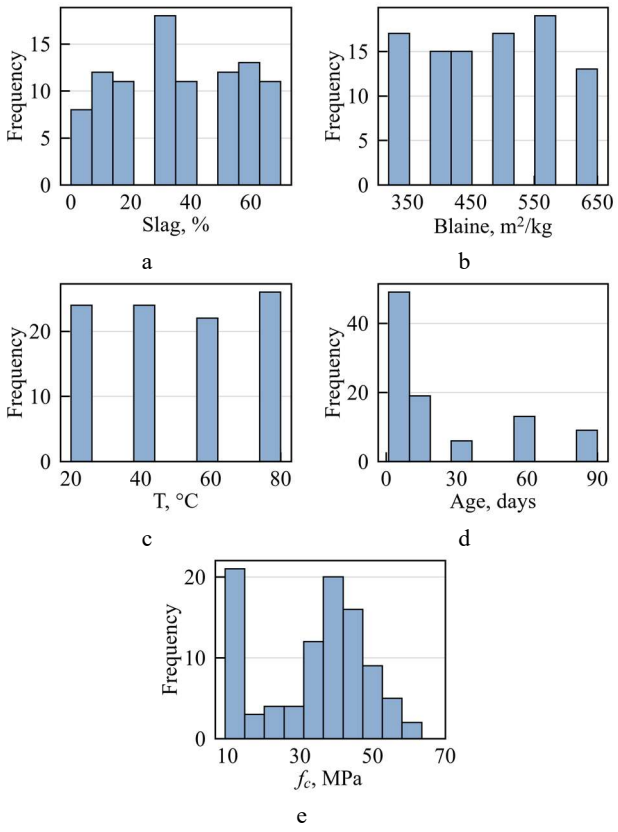


Fig. 1. Histograms of the four input variables of the assembled database (N = 96): a – slag replacement; b – Blaine fineness; c – curing temperature; d – age; e – the output variable (compressive strength)

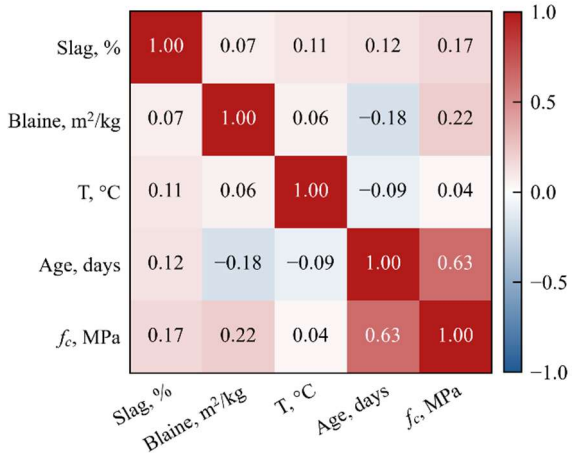


Fig. 2. Pearson correlation matrix between the input variables and the compressive strength of the activated slag mortars

The slag replacement ratio displays a weak positive linear correlation ($\rho \approx 0.17$), which reflects the competing effects of the reduced early-age reactivity of high-slag systems, their higher long-term strength gain, and the well-known optimum that lies in the 30 – 50 % replacement range [1, 3]. The low pairwise correlations between the four input variables ($|\rho| \leq 0.18$) confirm the absence of multicollinearity, allowing all four predictors to be retained in the subsequent modelling.

3. RESPONSE SURFACE METHODOLOGY

3.1. Mathematical model

Response surface methodology (RSM) is a collection of statistical and mathematical techniques used to model the relationship between several input variables and one or more responses, with the aim of optimising the response [2]. In this study, a second-order (quadratic) polynomial of the four input variables was fitted to the compressive strength data:

$$f_c = \beta_0 + \Sigma\, \beta_i\, x_i + \Sigma\, \beta_{ii}\, x_i^2 + \Sigma\Sigma\, \beta_i\, x_i x_j + \varepsilon\,, \qquad (1)$$

where β_0 is the intercept, β_i, β_{ii} and β_{ij} are the linear, pure-quadratic and two-factor interaction coefficients, respectively; x_i are the coded input variables (A = slag, B = Blaine, C = temperature, D = age); ε is the residual error. The model was identified by ordinary least squares (OLS) using the full 96-sample database, and statistical significance of the individual terms was assessed by analysis of variance (ANOVA) at $\alpha = 0.05$.

3.2. ANOVA and significance of terms

The ANOVA results for the second-order RSM model are reported in Table 2.

Table 2. ANOVA results for the second-order RSM model of compressive strength (only the significant and key marginal terms are listed)

Source	Sum of squares	df	F-value	p-value	Significance
A- slag, %	124.75	1	2.25	0.137	ns
B-Blaine, m²/kg	1490.66	1	26.94	< 0.001	***
C-T, °C	19.55	1	0.35	0.554	ns
D-age, days	8725.97	1	157.69	< 0.001	***
A²	127.50	1	2.30	0.133	ns
D²	4434.28	1	80.14	< 0.001	***
A × D	129.60	1	2.34	0.130	ns
Residual	4482.12	81	–	–	–
Total ($R^2 = 0.785$)	–	95	–	–	–

3.3. Response surface analysis

Three-dimensional response surfaces of the fitted RSM model are shown in Fig. 3 and Fig. 4 for the two most physically meaningful variable pairs (slag-age, Blaine-temperature).The surfaces clearly capture the rapid initial gain of compressive strength followed by a plateau at later ages, as well as the non-monotonic effect of slag replacement: the predicted optimum lies at intermediate replacement levels (≈ 40 – 50 %) at early and medium ages and moves towards higher replacement levels at later ages, in agreement with the optimum range reported in the literature for activated slag mortars [1]. The overall predictive accuracy of the RSM model is illustrated in Fig. 5, which plots the predicted against the experimental compressive strengths together with the ± 20 % deviation envelope.

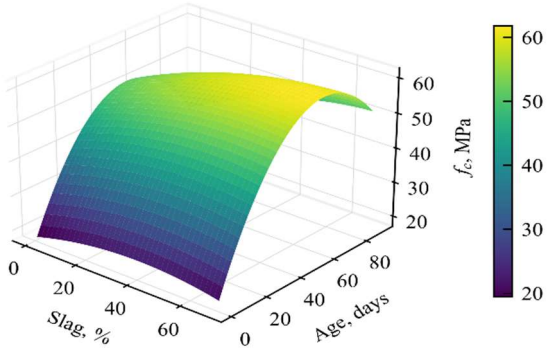


Fig. 3. RSM-predicted compressive strength as a function of slag replacement ratio and curing age (Blaine and temperature fixed at their median values)

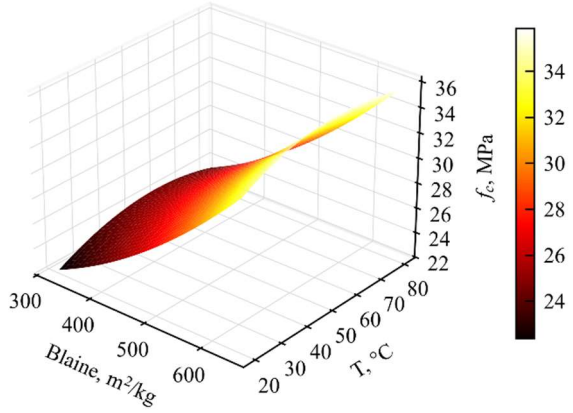


Fig. 4. RSM-predicted compressive strength as a function of slag Blaine fineness and curing temperature (slag and age fixed at their median values)

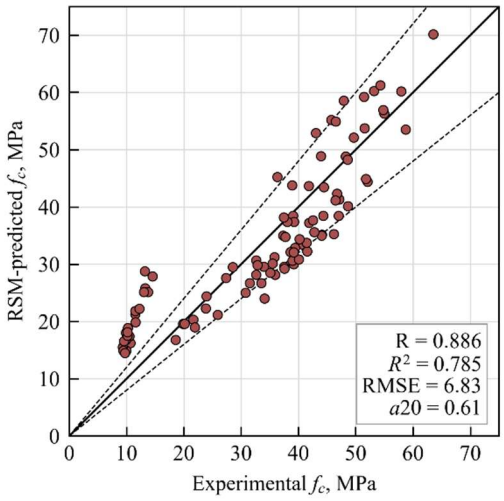


Fig. 5. Predicted versus experimental compressive strength for the second-order RSM model ($R^2 = 0.785$; dashed lines indicate the ± 20 % deviation envelope)

4. ARTIFICIAL NEURAL NETWORK MODELLING

4.1. Network architecture and training

A multilayer feed-forward back-propagation neural network was used to model the compressive strength as a non-linear mapping of the four input variables. The architecture (Fig. 6) is a 4-9-6-1 network with two hidden layers and hyperbolic-tangent (tanh) activation in the hidden layers. This topology was chosen after a trial-and-error procedure on hidden-layer sizes ranging from 1 to 30 neurons, in line with the architectures reported in [1, 2]. The network was trained with the Levenberg–Marquardt (LM) back-propagation algorithm, which is well suited to medium-sized networks ($\lesssim$ a few hundred weights; 112 weights and biases in the present case) and consistently outperformed quasi-Newton, resilient back-propagation and one-step secant alternatives in our preliminary tests, in agreement with [1, 2].

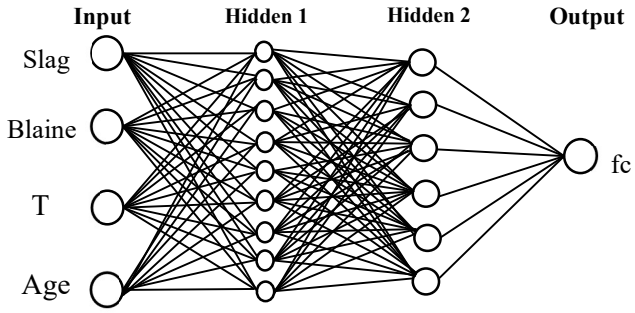


Fig. 6. Architecture of the proposed 4-9-6-1 back-propagation neural network for predicting the compressive strength of activated binary slag mortars

4.2. Data preparation

All input and output variables were normalised to the [0, 1] range using min–max scaling to mitigate the differing magnitudes of the predictors and accelerate convergence:

$$xnorm = \frac{x - xmi}{xmax - xmi}. \quad (2)$$

The 96-sample database was randomly partitioned into 70 % for training (67 samples), 15 % for validation (14 samples), and 15 % for testing (15 samples), following the splitting strategy adopted in [1, 2, 3]. Training was stopped when the validation error failed to decrease for 25 consecutive epochs (early stopping) and the weights at the epoch of minimum validation error were retained; the network with the lowest validation error among 20 independent random initialisations was selected as the optimum model. The optimisation criterion was the mean squared error:

$$MSE = \left(\frac{1}{N}\right) \Sigma\, (y_i - \hat{y}_i)^2, \quad (3)$$

where y_i and $\hat{y}_i$ are the measured and predicted strengths and N is the number of samples in the corresponding subset.

4.3. ANN performance

The convergence of the training loss is shown in Fig. 7. The training MSE decreases by more than two orders of magnitude within the first 11 epochs, where the validation error reaches its minimum ($\approx 9 \times 10^{-4}$). Beyond this point the validation error starts to increase while the training error keeps decreasing; the early-stopping criterion therefore terminated the training at epoch 36, and the weights of epoch 11 were retained to prevent overfitting.

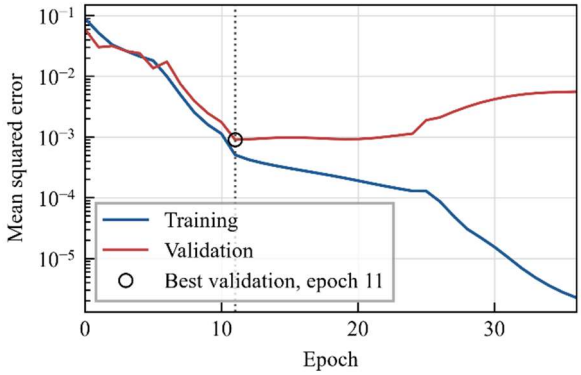


Fig. 7. Convergence of the mean squared error during training of the 4-9-6-1 ANN

The performance metrics, Pearson correlation coefficient R, coefficient of determination R^2, root-mean-square error (RMSE), mean absolute error (MAE) and the engineering a20-index defined in Eq. 4 are summarised in Table 3.

$$a20 - index = \frac{m20}{N}, \quad (4)$$

where $m20$ is the number of samples whose ratio of measured to predicted strength lies within the [0.80, 1.20] interval. A value of unity indicates a perfect match within ± 20 %.

Table 3. Performance metrics of the optimum 4-9-6-1 ANN on the training, validation, testing and combined data subsets

Subset	R	R^2	RMSE, MPa	MAE, MPa	a20-index
Training	0.9969	0.9938	1.221	0.922	1.000
Validation	0.9911	0.9814	1.627	1.267	1.000
Testing	0.9927	0.9803	1.785	1.356	1.000
All data	0.9957	0.9911	1.387	1.040	1.000

As shown in Fig. 8 and Fig. 9, all data points lie inside the ± 20 % envelope (a20-index = 1.00), and the ANN tracks the experimental strengths very closely across the entire 9 – 64 MPa range. The slight scatter observed at intermediate strengths (30 – 45 MPa) reflects the regions of the design space where the synergy between mechanical and thermal activation is strongest.

5. MODEL VALIDATION AND PERFORMANCE EVALUATION

5.1. Sensitivity analysis

To rank the four input variables by their relative importance for the compressive-strength response, a model-based sensitivity analysis was carried out on the trained ANN. Each variable was swept across its full normalised range while the other three were held fixed at every observed combination in the database, and the average peak-to-peak response was integrated to give a total-effect index:

$$SAi = \frac{\langle fmax(xi) - fmin(xi) \rangle}{\Sigma \langle \cdot \rangle} \times 100\ \%. \quad (5)$$

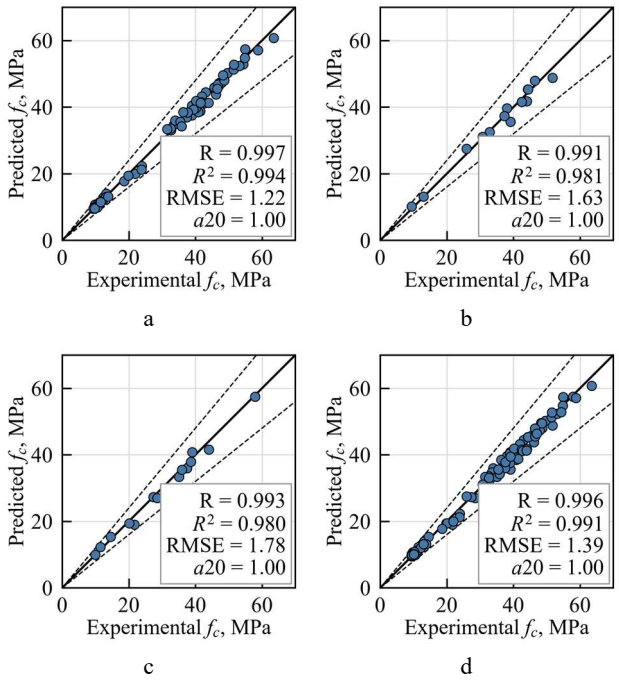


Fig. 8. Predicted versus experimental compressive strength for the 4-9-6-1 ANN: a – training; b – validation; c – testing; d – all data. Dashed lines indicate the ± 20 % deviation envelope

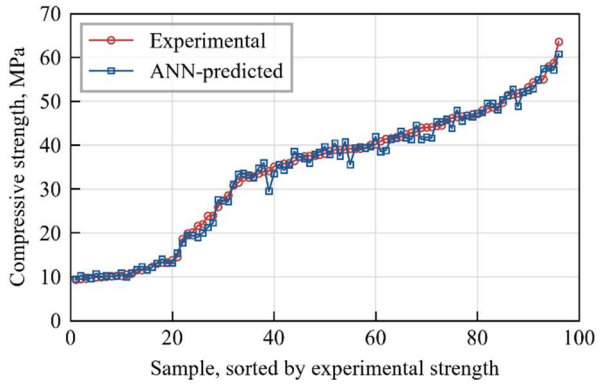


Fig. 9. Sample-by-sample comparison between the experimental compressive strengths and the values predicted by the optimum ANN model (samples sorted by ascending experimental strength)

The corresponding ranking is shown in Fig. 10: curing age dominates the response (≈ 66 %), followed by slag fineness (≈ 22 %), curing temperature (≈ 6 %) and slag replacement ratio (≈ 5 %). This ranking is in agreement with the basic phenomenology of activated slag systems: hydration is fundamentally a time-dependent process, and once the slag has been finely ground (i.e., once the available reactive surface has been increased), the strength evolves predominantly with age, with thermal activation only modulating the rate.

5.2. Comparison between RSM and ANN

Table 4 summarises the global accuracy metrics of the two models on the full 96-sample dataset. The ANN clearly outperforms the second-order RSM polynomial: the ANN achieves a coefficient of determination of 0.991 and an RMSE of 1.39 MPa, against 0.785 and 6.83 MPa for the RSM model.

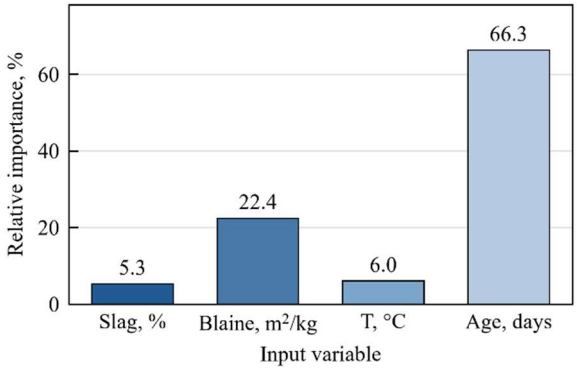


Fig. 10. Relative importance of the four input variables on the compressive strength of activated slag mortars, computed from the trained ANN using the total-effect sensitivity index of Eq. 5

Table 4. Global comparison between the second-order RSM and the 4-9-6-1 ANN on the full 96-sample database

Metric	RSM	ANN
R	0.886	0.996
R^2	0.785	0.991
RMSE, MPa	6.83	1.39
MAE, MPa	5.93	1.04
a20-index	0.61	1.00

The a20-index of the ANN is 1.00, while the RSM model only places 61 % of its predictions inside the ± 20 % envelope. This is consistent with the findings of Li et al. [2], who reported that an ANN clearly outperformed an RSM model for high-strength concrete (R^2 = 0.998 vs 0.963), and with the conclusions of Apostolopoulou et al. [1] for cement- and lime-metakaolin mortars.

6. DISCUSSION

The results reported in Sections 3 – 5 confirm that the strength evolution of activated binary slag mortars is intrinsically non-linear and that a quadratic RSM model, although mathematically simple and easy to interpret through ANOVA, cannot describe the full range of mix-curing combinations. About 40 % of the residual sum of squares of the RSM model originates from the early-age records ($t \leq 3$ days, 30 of the 96 samples), where the rapid hyperbolic strength gain is poorly approximated by a polynomial of degree two. By contrast, the ANN naturally accommodates this hyperbolic behaviour because of its non-linear activation functions, and the use of two hidden layers allows it to capture the synergy between mechanical and thermal activation that classical regression cannot easily represent. From a physico-chemical standpoint, this non-linearity mirrors the hydration mechanism of GGBFS itself. Unlike OPC, slag hydration is not diffusion-controlled from the outset: it first requires the glassy aluminosilicate network to be depolymerised by hydroxide ions released during cement hydration, after which C-(A)-S-H gel with a lower Ca/Si ratio and a more disordered, cross-linked structure than OPC-derived C-S-H begins to precipitate and

progressively fills the capillary pore space. Because this depolymerisation step has to occur before bulk strength gain can proceed, the early-age response is inherently delayed and then accelerates sharply once a percolating gel network forms, a threshold-and-acceleration behaviour that a smooth second-order polynomial cannot reproduce but that the ANN's non-linear hidden units approximate naturally. Mechanical activation (finer Blaine fineness) shortens this induction period by increasing the specific surface available for dissolution, which is consistent with its position as the second most influential variable in the sensitivity ranking. Thermal activation accelerates the same dissolution-precipitation kinetics but, above roughly 60 °C, tends to promote a coarser, more heterogeneous C-(A)-S-H microstructure with higher capillary porosity, which offsets part of the kinetic gain and explains its comparatively modest and non-monotonic contribution to long-term strength.

The dominance of curing age (≈ 66 %) and slag fineness (≈ 22 %) in the sensitivity ranking is in line with the chemistry of activated slag systems. Mechanical activation increases the reactive specific surface and accelerates the dissolution of the glassy slag phase, while age controls the cumulative degree of reaction. Thermal activation has a smaller relative weight (≈ 6 %) because, beyond a critical temperature (≈ 60 °C), the additional gain in reaction rate is partially offset by coarsening of the C–(A)–S–H gel and increased porosity, so its net effect on long-term strength is moderate.

From a mix-design perspective, the trained ANN can be used as a fast surrogate to identify the activation regime that maximises strength for a given target. Parametric predictions of both models (cf. Fig. 3) indicate, in particular, that the optimum slag replacement at 28 days under standard 20 °C curing lies at intermediate levels (≈ 25 – 50 %) and shifts towards higher replacement levels when thermal activation at 60 °C is applied or when the curing age increases, a consistent trend recovered by both models.

The performance of the ANN reported here ($R^2 = 0.991$) is comparable to the values reported by Apostolopoulou et al. [1] for a 7-9-27-1 BPNN trained on 298 metakaolin-lime/cement mortars ($R = 0.998$), by Li et al. [2] for a 5-input ANN on 324 high-strength concrete records ($R^2 = 0.998$) and by Al-Jamimi et al. [3] for an SVM-GA model on 108 plain and blended cement concretes ($R^2 = 0.99$). The fact that a comparable accuracy is reached with only 96 samples confirms the value of carefully curated datasets and well-tuned compact architectures.

It is important to acknowledge two limitations. First, the database covers a limited range of cement and slag chemistries; extrapolation to more exotic activators (alkali-activated systems, sulfate activation, very high MgO slags) requires retraining. Second, the present model targets cube compressive strength only; durability indicators such as chloride permeability or carbonation depth, which are equally critical for SCM-based binders [3], are not captured here and constitute a natural extension of this work.

7. CONCLUSIONS

This study has presented a comparative assessment of response surface methodology (RSM) and artificial neural network (ANN) models for predicting the compressive strength of activated binary slag mortars on a unified database of 96 mix-curing combinations. The main conclusions are as follows:

1. The 4-9-6-1 back-propagation ANN trained with the Levenberg–Marquardt algorithm reproduces the experimental compressive strengths with $R = 0.996$, $R^2 = 0.991$, RMSE = 1.39 MPa and an a20-index of 1.00 over the full 1- to 90-day curing range.
2. The quadratic RSM polynomial gives a much lower global accuracy ($R^2 = 0.785$, RMSE = 6.83 MPa, a20-index = 0.61) and is unable to capture the hyperbolic early-age strength gain. Its main practical role is therefore the identification, through ANOVA, of the statistically dominant terms, in this case the linear and quadratic effects of curing age and the linear effect of Blaine fineness ($p < 0.001$).
3. Sensitivity analysis on the trained ANN ranks the four input variables as follows: curing age ≈ 66 %, slag Blaine fineness ≈ 22 %, curing temperature ≈ 6 % and slag replacement ratio ≈ 5 %. Mechanical activation of the slag (increased fineness) is therefore the second strongest lever after age, while thermal activation has a more modest effect.
4. The ANN can be used as a fast surrogate for mix-design optimisation, indicating that the optimum slag replacement lies at intermediate levels (≈ 25 – 50 % at 28 days under standard curing) and shifts towards higher replacement levels under thermal activation (60 °C) and at later ages.
5. Future work will extend the database to alkali-activated and ternary systems and incorporate durability indicators (chloride permeability, carbonation, drying shrinkage) into a multi-output network.

Acknowledgments

The authors acknowledge the institutions whose published experimental data made the construction of the unified database possible. No external funding was received for this work.

REFERENCES

1. **Apostolopoulou, M., Douvika, M.G., Kanellopoulos, I.N., Moropoulou, A., Asteris, P.G.** Prediction of Compressive Strength of Mortars using Artificial Neural Networks *Proceedings of the 1st International Conference TMM_CH on Transdisciplinary Multispectral Modelling and Cooperation for the Preservation of Cultural Heritage* 2019: pp. 269 – 281.
2. **Li, T., Yang, J., Jiang, P., AlAteah, A.H., Alsubeai, A., Alfares, A.M., Sufian, M.** Predicting High-Strength Concrete's Compressive Strength: A Comparative Study of Artificial Neural Networks, Adaptive Neuro-Fuzzy Inference System, and Response Surface Methodology *Materials* 17 (18) 2024: pp. 4533. https://doi.org/10.3390/ma17184533
3. **Al-Jamimi, H.A., Al-Kutti, W.A., Alwahaishi, S., Alotaibi, K.S.** Prediction of Compressive Strength in Plain and Blended Cement Concretes Using a Hybrid Artificial Intelligence Model *Case Studies in Construction Materials* 17 2022: pp. e01238. https://doi.org/10.1016/j.cscm.2022.e01238

4. **Asteris, P.G., Kolovos, K.G., Douvika, M.G., Roinos, K.** Prediction of Self-compacting Concrete Strength Using Artificial Neural Networks *European Journal of Environmental and Civil Engineering* 20 (1) 2016: pp. s102 – s122. https://doi.org/10.1080/19648189.2016.1246693
5. **Sarıdemir, M.** Predicting the Compressive Strength of Mortars Containing Metakaolin by Artificial Neural Networks and Fuzzy Logic *Advances in Engineering Software* 40 (9) 2009: pp. 920 – 927. https://doi.org/10.1016/j.advengsoft.2008.12.008
6. **Eskandari-Naddaf, H., Kazemi, R.** ANN Prediction of Cement Mortar Compressive Strength, Influence of Cement Strength Class *Construction and Building Materials* 138 2017: pp. 1 – 11. https://doi.org/10.1016/j.conbuildmat.2017.01.132
7. **Hammoudi, A., Moussaceb, K., Belebchouche, C., Dahmoune, F.** Comparison of Artificial Neural Network (ANN) and Response Surface Methodology (RSM) Prediction in Compressive Strength of Recycled Concrete Aggregates *Construction and Building Materials* 209 2019: pp. 425 – 436. https://doi.org/10.1016/j.conbuildmat.2019.03.119
8. **Worrell, E., Price, L., Martin, N., Hendriks, C., Meida, L.O.** Carbon Dioxide Emissions from the Global Cement Industry *Annual Review of Energy and the Environment* 26 (1) 2001: pp. 303 – 329. https://doi.org/10.1146/annurev.energy.26.1.303
9. **Behnood, A., Golafshani, E.M.** Predicting the Compressive Strength of Silica Fume Concrete Using Hybrid Artificial Neural Network with Multi-Objective Grey Wolves *Journal of Cleaner Production* 202 2018: pp. 54 – 64. https://doi.org/10.1016/j.jclepro.2018.08.065
10. **Yeh, I.C.** Modeling of Strength of High-Performance Concrete Using Artificial Neural Networks *Cement and Concrete Research* 28 (12) 1998: pp. 1797 – 1808. https://doi.org/10.1016/S0008-8846(98)00165-3



© Boualleg et al. *2027* Open Access This article is distributed under the terms of the Creative Commons Attribution 4.0 International License (http://creativecommons.org/licenses/by/4.0/), which permits unrestricted use, distribution, and reproduction in any medium, provided you give appropriate credit to the original author(s) and the source, provide a link to the Creative Commons license, and indicate if changes were made.